

ApJ, in press.

On the origin of black hole X-ray emission in quiescence: *Chandra* observations of XTE J1550–564 and H 1743–322 .

S. Corbel¹, J.A. Tomsick², P. Kaaret³

ABSTRACT

We report the results of observations of the black hole binaries XTE J1550–564 and H 1743–322 in their quiescent state using the *Chandra X-ray Observatory*. Both sources are detected at their faintest level of X-ray emission ever observed with a 0.5–10 keV unabsorbed luminosity of 2×10^{32} $(d/5 \text{ kpc})^2 \text{ erg s}^{-1}$ for XTE J1550–564 and $9 \times 10^{31} (d/8 \text{ kpc})^2 \text{ erg s}^{-1}$ for H 1743–322. These luminosities are in the upper range compared to the faintest levels observed in other black hole systems, possibly related to residual accretion for these sources with frequent outbursts. For XTE J1550–564, the *Chandra* observations also constrain the X-ray spectrum as a fit with an absorbed power-law model yields a photon index of 2.25 ± 0.08 , clearly indicating a softening of the X-ray spectrum at lower luminosities compared to the standard hard state. Similar softening at low luminosity is seen for several black hole transients with orbital periods less than 60 hours. Most of the current models of accreting black holes are able to reproduce such softening in quiescence. In contrast, we find that systems with orbital periods longer than 60 hours appear to have hard spectra in quiescence and their behaviour may be consistent with hardening in quiescence.

Subject headings: accretion, accretion disks – black hole physics – stars: individual (H 1743–322, XTE J1550–564) – X-rays: binaries

¹AIM - Unité Mixte de Recherche CEA - CNRS - Université Paris VII - UMR 7158, CEA Saclay, Service d’Astrophysique, F-91191 Gif sur Yvette, France.

²Center for Astrophysics and Space Sciences, University of California at San Diego, MS 0424, La Jolla, CA92093, USA.

³Department of Physics and Astronomy, University of Iowa, Iowa City, IA 52242 USA.

1. Introduction

X-ray Novae (or Soft X-ray Transients) are compact binaries in which a neutron star or black hole (BH) primary accretes from a donor star via Roche-lobe over-flow. Most of these systems are usually in a quiescent state with an X-ray luminosity of 10^{30} to 10^{33} erg s $^{-1}$. However, they undergo episodic outbursts that last for months with X-ray luminosities that can sometime reach or exceed the Eddington limit ($\sim 10^{39}$ erg s $^{-1}$ for a $10 M_{\odot}$ BH). Despite the residual activity of these quiescent objects, very little is known about their emission properties at very low accretion rates (McClintock & Remillard 2005). With the sensitivity of current X-ray missions (in particular *Chandra* and *XMM-Newton*), it is now possible to study in more detail the physical processes that take place in this accretion regime.

XTE J1550–564 was discovered by *RXTE*/ASM on 1998 September 7 (Smith 1998). A brief and intense radio/X-ray flare, associated with a massive plasma ejection, was observed two weeks later (Hannikainen et al. 2001). Subsequent radio and X-ray observations revealed the formation of large scale jets moving away from the XTE J1550–564 black hole over the course of several years (Corbel et al. 2002; Tomsick et al. 2003a; Kaaret et al. 2003). After its discovery outburst in 1998–1999, XTE J1550–564 had a second strong outburst in 2000, and fainter and shorter outbursts were detected in 2001, 2002 and 2003 (Figure 1). Optical observations indicate that the compact object in XTE J1550–564 is likely a black hole of $10.5 \pm 1.0 M_{\odot}$ at a distance of about 5.3 kpc (Orosz et al. 2002).

H 1743–322 was discovered with *Ariel V* in August 1977 (Kaluzienski & Holt 1977) and was precisely localized by *HEAO-1* a few weeks later (Doxsey et al. 1977). Based on its X-ray properties, H 1743–322 has been classified as a black hole candidate (White & Marshall 1983). In March 2003, *INTEGRAL* detected new activity from IGR J17464–3213 (Revnivtsev et al. 2003) that was later found to correspond to H 1743–322. During outburst, H 1743–322 went through several X-ray states with properties typical of BHC. The 2003 outburst ended around late November 2003. H 1743–322 was observed again in outburst from July 2004 (Swank 2004) to November 2004. A bright radio flare (likely associated with a massive ejection event) was observed in 2003 by Rupen et al. (2003). The ejected plasma was later found to interact with the interstellar medium causing in-situ particle acceleration and the formation of two large-scale, synchrotron-emitting radio and X-ray jets (Corbel et al. 2005) as in the XTE J1550–564 case.

In this paper, we present the results of ten *Chandra* observations of the two black holes XTE J1550–564 and H 1743–322 carried out during their quiescent state. These two sources have been detected at their faintest level ever observed. The high quality *Chandra* spectra for XTE J1550–564 allow us to study and monitor the emission properties of this black hole at very low accretion rate. We then investigate the quiescent emission of black hole systems.

2. Observations and data reduction

Our *Chandra* program of monitoring X-ray jets from XTE J1550–564 and H 1743–322 has also allowed us to study in great detail the black holes in these two systems. XTE J1550–564 was observed by *Chandra* on five occasions: 2002 March 11 (MJD 52344.8), 2002 June 19 (MJD 52444.5), 2002 September 24 (MJD 52542.0), 2003 January 27 (MJD 52667.3) and 2003 October 23 (MJD 52935.6). For completeness, we also include the results of two published *Chandra* observations on 2000 August 21 (MJD 51777.4) and 2000 September 11 (MJD 51798.3) that were performed during the decay of the 2000 outburst of XTE J1550–564 (Tomsick et al. 2001). The *Chandra* observations of H 1743–322 were carried out on three occasions: 2004 February 12 (MJD 53048), March 24 (MJD 53089) and March 27 (MJD 53092). Figure 1 shows the *RXTE*/ASM 1.5–12 keV light-curves of XTE J1550–564 and H 1743–322, and the arrows indicate the dates of the *Chandra* observations. This illustrates that all our observations were conducted a few months (or even up to a year for XTE J1550–564) after or before a period of significant X-ray activity (outburst). This allows us to monitor the emission properties of XTE J1550–564 and H 1743–322 during their quiescent phases.

For all *Chandra* observations, we used the Advanced CCD Imaging Spectrometer spectroscopic array (ACIS-S; Bautz et al. 1998) in imaging mode, with the target placed on one of the back-illuminated ACIS Chips (S3). For the first observation of XTE J1550–564 in 2002 and the first observation of H 1743–322, only the S3 chip was read out and a 1/2 sub-array mode was used to limit pile-up. For the later observations, the sources were known to be at lower flux and the full ACIS-S imaging mode array was used.

We produced 0.3–8 keV ACIS images using the “level 2” event lists from the standard data processing using the *Chandra* Interactive Analysis of Observations (CIAO) software package. We constructed light curves with all valid events on the S3 chips to search for times of high background. Periods with background flares were removed using the standard CIAO script *analyse_ltcrv.sl*. We searched for X-ray sources in each 0.3–8 keV image using *wavdetect* (Freeman et al. 2002), the wavelet-based source detection routine in CIAO. For all *Chandra* observations, an X-ray source is found at the location of the black hole. With an absolute astrometric precision of 0.6'' (90% confidence level), the *Chandra* locations are consistent with the positions reported at other wavelengths (see also Corbel et al. 2005 for H 1743–322). As the focus of this paper is the spectra of the two black holes in quiescence, we refer the reader to the studies of the X-ray jets presented in Corbel et al. (2002; 2005), Tomsick et al. (2003a), Kaaret et al. (2003) as well as the Tomsick et al. (2001) black hole study for details of the *Chandra* data reduction.

3. Spectral properties of XTE J1550–564 and H 1743–322 in quiescence

We extracted energy spectra in the 0.3–8 keV energy range for the black holes in all *Chandra* observations using CIAO tools, and we fitted these spectra using XSPEC. We used a circular source extraction region with radii of 1.4" and 4", for H 1743–322 and XTE J1550–564, respectively. We extracted background spectra from annuli with inner radii of 9" and 6" and outer radii of 19" and 16" for H 1743–322 and XTE J1550–564, respectively. These regions were centered on the black hole positions as given by *wavdetect*. The source aperture size is adapted to enclose most of the source counts. Background region are adapted to cover a sufficiently large empty region. Due to the low numbers of source counts for H 1743–322 (52 counts or less), we used the W statistic for fitting (Wachter et al. 1979; Arnaud, in prep.) the un-binned spectra. This is adapted from the Cash statistic (Cash 1979) and is valid for background subtracted spectra. For XTE J1550–564, which is brighter than H 1743–322, we re-binned the spectra in order to have enough counts in each bin to be able to use the χ^2 statistic (with the exception of the *Chandra* observations on MJD 51777, 51798 and 52444, for which we used the W statistic due to the low number of counts).

These spectra are adequately fitted with a power-law model including interstellar absorption. We used this model because this spectral shape is typically seen for black holes in quiescence (Garcia et al. 2001; Kong et al. 2002), but we emphasize that we can not statistically rule out other spectral shapes. However, bremsstrahlung models provide un-physical temperatures as already mentioned in Kong et al. (2002). For H 1743–322, we fixed the equivalent hydrogen absorption column density, N_H to the constant value ($2.3 \times 10^{22} \text{ cm}^{-2}$) measured in *Chandra* observations of H 1743–322 during its 2003 outburst (Miller et al. 2005). For XTE J1550–564, we left N_H as a free parameter in our fit. As the values obtained (Table 1) are consistent with results from previous X-ray outbursts ($9 \times 10^{21} \text{ cm}^{-2}$; Tomsick et al. 2001), we also fixed the column density of XTE J1550–564 to this value. This column density is inconsistent with the value inferred from the interstellar absorption lines (Sánchez-Fernández et al. 1999), but agrees with the hydrogen column density deduced from X-ray spectra of XTE J1550–564 or its associated X-ray jets (Tomsick et al. 2001, 2003a; Kaaret et al. 2003), and also with the Galactic column density along the line of sight (Jain et al. 1999). The difference when compared to the optical measurement of Sánchez-Fernández et al. (1999) may be explained in various ways. One possibility is that the X-ray absorption column density may be intrinsically higher than the optically-inferred value due to additional local material covering the X-ray source. Another possibility is that the absorption column density deduced from the interstellar absorption lines are artificially lower (due to saturation for example, Hynes et al. 2004). We believe that the latter is more likely as XTE J1550–564 and its X-ray jets (which are separated by up to 30") have similar

column densities. In addition, it is interesting to point out the absence of variation of the hydrogen column density between outburst and quiescence.

For H 1743–322, the best-fit photon indices are $1.3_{-1.7}^{+2.1}$, $1.6_{-1.3}^{+1.0}$ and 2.2 ± 0.6 for the observations on MJD 53048, 53089 and 53091, respectively. Refitting these three data sets simultaneously (allowing the normalization to vary) leads to a photon index of 1.96 ± 0.46 (with 90% confidence errors). As there are more frequent observations of XTE J1550–564, its X-ray spectrum is better constrained. The fit results of the individual observations are reported in Table 1. To provide the best constraint on the spectral parameters, we simultaneously fit all seven datasets simultaneously (again allowing the normalization to vary). Leaving the hydrogen column density as a free parameter leads to $N_H = (8.8 \pm 1.0) \times 10^{21} \text{ cm}^{-2}$, which is consistent with previous estimates. With N_H frozen to $9 \times 10^{21} \text{ cm}^{-2}$ (Tomsick et al. 2001), we obtain the best constraint on the photon index for XTE J1550–564 in quiescence, $\Gamma = 2.25 \pm 0.08$ (with 90% confidence errors). Figure 2 shows the 68%, 90% and 99% error contours allowing two parameters (N_H and Γ) to vary. The results indicate that these parameters are very well constrained by our observations.

The photon indices in all *Chandra* observations of XTE J1550–564 (Figure 3) are consistent with the value obtained by fitting the spectrum from the observation with the brightest flux (on MJD 52345) alone. This indicates that the X-ray spectra of XTE J1550–564 are consistent with the same spectral shape for all the observations, even though the flux varies by a factor of at least 16.

The fact that the X-ray flux varies between the observations indicates that accretion onto the black hole has not stopped in quiescence. We use the *Chandra* observations of XTE J1550–564 on MJD 52344 to construct a light-curve of XTE J1550–564 with a time resolution of 1 ks (Figure 4). A fit with a constant level leads to a χ^2 of 74 for 27 degrees of freedom, clearly indicating that there is also significant X-ray variability on short (\sim ks) time-scale.

The un-absorbed 0.5–10 keV fluxes for H 1743–322 and XTE J1550–564 are reported in Table 1. For H 1743–322, we fixed the power-law photon index to a value of 2.0, whereas for XTE J1550–564, the photon index was left at its fitted value. For both sources, the column densities were fixed as indicated previously. The quoted errors are based on the numbers of source and background counts and Poisson statistics.

4. Discussion

4.1. X-ray luminosity in quiescence

These *Chandra* observations represent the detection of XTE J1550–564 and H 1743–322 at their faintest level of X-ray emission. The un-absorbed 0.5–10 keV luminosity of XTE J1550–564 is 1.9×10^{32} erg s $^{-1}$ (for a distance of 5.3 kpc, Orosz et al. 2002) and 9.3×10^{31} erg s $^{-1}$ for H 1743–322 (at a distance of 8 kpc). For a ten solar mass black hole, these values correspond to luminosities of 1.5×10^{-7} L_{Edd} (for XTE J1550–564) and 7.2×10^{-8} L_{Edd} (for H 1743–322). We note that the mass of the compact object in H 1743–322 is unknown, as well as its distance. However, the kinematic study of the large scale jets of H 1743–322, as well as its location toward the Galactic bulge, are consistent with a distance to H 1743–322 of 8 kpc (Corbel et al. 2005).

These quiescent luminosity levels are in the upper range compared to the the faintest detected levels of other black holes (Garcia et al. 2001, Kong et al. 2002, Sutaria et al. 2002, Hameury et al. 2003, Tomsick et al. 2003b). We note that there is still the possibility that these sources were not observed in their true quiescent levels as the *Chandra* observations were carried out between outbursts. However, we note that for XTE J1550–564, the *Chandra* observations took place during three distinct quiescent phases (Figure 1) and a similar quiescent X-ray level is detected for two of these phases. In addition, optical observations (Jain et al. 2001) confirm that XTE J1550–564 returned to quiescence on a timescale of months. For H 1743–322, we note that the last two *Chandra* observations were taken 2.5 days apart. The flux in the observation on MJD 53089 is consistent with the flux observed during the first *Chandra* observation taken 40 days before, which indicates that this is probably the quiescent level of H 1743–322. Between the second and third *Chandra* observations, the flux more than doubled in less than three days. This may be related to continuous accretion in quiescence or possibly means that this could be the onset of the outburst that was detected by *RXTE*/ASM about 90 days later (Swank 2004). Similarly, RXTE/PCA detected the X-ray activity of GX 339–4 during its 2002 outburst at least 40 days before the initial ASM detection (Homan et al. 2005). This probably indicates that the *Chandra* observations at the lowest level are likely representative of the true quiescent phase of XTE J1550–564 and H 1743–322 .

4.2. X-ray spectra and photon index in quiescence

In addition to allowing for detection of these two black holes in quiescence, for XTE J1550–564 these observations also provide the most precise X-ray spectra of a black hole at such low

luminosities (down to $\sim 10^{-7} L_{\text{Edd}}$). We concentrate on the power-law model, which can be representative of various emission mechanisms (see section 4.4). With a photon index of 2.25 ± 0.08 , the X-ray spectra of XTE J1550–564 are significantly softer than during the standard hard state (photon index of the order of 1.5 to 1.7; Tomsick et al. 2001). This trend was marginally apparent in the decay of the 2000 outburst of XTE J1550–564 (Tomsick et al. 2001), but our *Chandra* observations of XTE J1550–564 clearly confirm this softening in quiescence.

In fact, this is very similar to several other black holes for which an X-ray spectrum has been measured in quiescence. For the rest of this paper, we will concentrate on those systems for which the photon index has been measured with relatively high precision. We have collected results from the literature which are presented in Table 2 (90% confidence level for the uncertainty on the photon indices) and in Figures 5 and 6. The X-ray spectrum of XTE J1118+480 ($\Gamma = 2.02 \pm 0.16$) in quiescence (McClintock et al. 2003) is also softer than during its standard hard state ($\Gamma = 1.7$; Frontera et al. 2003). When GX 339–4 is detected at very low X-ray flux (Corbel et al. 2003; Gallo et al. 2003b; Chapuis et al. in prep.), the X-ray spectra are again consistent with being soft ($\Gamma = 1.99 \pm 0.15$; Chapuis et al. in prep) like XTE J1550–564 or XTE J1118+480. Similar conclusions can be drawn for A 0620–00, which has a photon index of 2.26 ± 0.18 in quiescence (McClintock et al. 2003). However, the X-ray spectra of a subset of sources stay hard or harden significantly in quiescence compared to the standard hard state: V404 Cyg ($\Gamma = 1.55 \pm 0.07$ with N_{H} frozen to optical value; Kong et al. 2002) and V4641 Sgr ($\Gamma = 0.2 \pm 0.9$; Tomsick et al. 2003b). With a photon index of $1.30_{-0.41}^{+0.34}$ (Hameury et al. 2003), GRO J1655–40 may also be considered as being hard in quiescence.

It is interesting to note that the three BHs with the hardest X-ray spectra in quiescence are those with the largest orbital period (Fig. 5). From our sample, all X-ray spectra from quiescent BHs with orbital period of less than two days are consistent with a soft power-law, whereas above this limit the power-law is hard. The weighted average photon index for the four “soft” sources is $\Gamma = 2.18 \pm 0.06$, whereas $\Gamma = 1.53 \pm 0.07$ for the three “hard” sources. The difference between the two samples is significant at more than seven σ , clearly indicating that the photon index may depend on the orbital period. However, our sample only includes seven sources with the hard sample dominated by V404 Cyg, and it needs to be confirmed by further observations of BHs in quiescence. GRS 1915+105, with an orbital period of 833 hours, would be a very good target if it returns to quiescence.

But as noted for XTE J1550–564 (section 3), the knowledge of the interstellar absorption column density is an important parameter for fitting the X-ray spectra. Indeed, lower column density leads to harder spectra (Fig. 5 in Kong et al. 2002). Some of the photon

indices quoted above are deduced from X-ray spectra with a fixed column density. We should now look if fixing the interstellar absorption could lead to an artificial bias in our sample. For XTE J1550–564 (this work) and GX 339–4 (Chapuis et al. in prep.), the deduced N_{H} (as a free parameter) is consistent with previous measurements. For XTE J1118+480 and A 0620–00, McClintock et al. (2003) used a fixed column density; however, as N_{H} is already very low for both of these sources, higher values would lead to even softer spectra. The X-ray and optical values of N_{H} for A 0620–00 and XTE J1118+480 are consistent with each other (Kong et al. 2002, McClintock et al. 2003). For GRO J1655–40 (Hameury et al. 2003) and V404 Cyg (Kong et al. 2002), X-ray fitting may indicate a slightly higher N_{H} when compared to the optical measurement. With N_{H} free, the photon indices are softer with $\Gamma = 1.54^{+1.2}_{-0.7}$ for GRO J1655–40 and $\Gamma = 1.81 \pm 0.14$ for V404 Cyg. For V4641 Sgr, there is no independent measurement of the X-ray column density due to the very fast transient nature of the source. To summarize, if we take into account the influence of the uncertain interstellar absorption column densities on the determination of the photon indices, the difference in photon indices is significant at the three sigma level.

If this trend is confirmed, it is of interest to understand the possible difference between the short and long orbital period systems. As outlined in Menou et al. (1999 and references therein), one of the obvious differences is the mass transfer rate between the companion star and the accretion disk. Indeed, following Frank et al. (1992), for Roche-lobe overflow systems, the mass transfer rate may be driven by two separate mechanisms: loss of angular momentum through gravitational radiation and magnetic braking (j-driven systems) or expansion of the donor star as it evolves away from the main sequence (n-driven systems). The j-driven systems would be found preferentially in short orbital period systems. The bifurcation period between these two populations is expected in the range 0.5–2 days (Menou et al. 1999). Interestingly, Menou et al. (1999) have estimated the mass transfer rate for typical binary-evolution models (see their figure 3) driven by gravitational radiation and by secondary expansion. If we compare the orbital period of the sources in our sample ($4.1 \text{ hrs} < P_{\text{orb}} < 155.3 \text{ hrs}$), we observe that systems with orbital periods in the range 4–30 hrs would have similar mass transfer rates to within a factor of a few. In any case, the systems with the longest orbital period would have a much higher mass transfer rate, and therefore, this could be an origin of the possible difference in photon indices.

Taking into account the mass of the black hole (Orosz 2003 and references therein), we can further look (Fig. 6) to see if a correlation exists between the power-law photon indices and the quiescent X-ray luminosities (expressed in Eddington units). The X-ray fluxes used in this graph are from Table 2 and represents the lowest level of X-ray emission reported for these sources. This figure illustrates that the sources with the softer or harder spectra do not occur in a specific luminosity range.

4.3. X-ray spectra at intermediate luminosities

Most of the X-ray Novae have not been observed/detected in X-rays in their quiescent state. However, we note that the softening of their X-ray spectra has been seen at flux level well above quiescence. In the decay phase of their recent outburst, XTE J1650–500 (Corbel et al 2004), as well as XTE J1908+094 (Jonker et al. 2004), are first observed to harden significantly in the hard state (we note that this is also the case for GX 339–4 at intermediate luminosity, possibly related to Compton reflection, Nowak et al. 2002). However, a clear softening ($\Gamma = 1.96 \pm 0.09$), like in GX 339–4, is then observed in XTE J1650–500 in the decay at a luminosity of 2×10^{34} erg s $^{-1}$ (Tomsick et al. 2004). No information is available on the quiescent spectra of XTE J1650–500 or XTE J1908+094, but it would be interesting to see if they also soften (as GX 339–4) in quiescence. Similarly, 4U 1543–47 gradually softened at intermediate luminosity ($\Gamma = 2.22 \pm 0.12$), whereas the hardest spectra in the hard state had $\Gamma = 1.64$ (Kalemci et al. 2005). *XMM-Newton* confirmed this softening with a photon index of $\Gamma = 1.94 \pm 0.04$ at a luminosity level of 4×10^{34} erg s $^{-1}$ ($10^{-5} L_{\text{Edd}}$) (La Palombara & Mereghetti (2005)). 4U 1543–47 was not in its true X-ray quiescence phase (at the time of the *XMM-Newton* observation) which is believed to occur below 3×10^{31} erg s $^{-1}$ (Garcia et al. 2001). However, the optical/infra-red monitoring (Buxton & Bailyn 2004) indicates that 4U 1543–47 reached its quiescent optical level only ten days after the *XMM-Newton* observations. It is unlikely that the X-ray flux could have decayed by three orders of magnitude on timescale of ten days. This may possibly point out that the optical emission settled down to its quiescent level much before the X-rays. Other examples of similar softening at intermediate luminosity during the decay phase include XTE J1748–288 (Kotani et al. 2000) and GS 1124–68 (Ebisawa et al. 1994).

4.4. On the X-ray emission of black holes in quiescence

One of the main results from our study is that a significant fraction of BHs have an X-ray spectrum that softens at lower luminosity. The emission of quiescent BHs is usually consistent with an extension of the hard state properties to lower luminosities (Corbel et al. 2000, 2003; Kong et al. 2000; Tomsick et al. 2004), and hard state models have been applied to explain the emission in the quiescent state.

Among these models, McClintock et al. (2003) explained the power-law photon index of $\Gamma = 2.02 \pm 0.16$ of XTE J1118+480 (one of the best studied black holes in quiescence) with an advection dominated accretion flow (ADAF) located inside a truncated standard thin disk. However, a pure ADAF model was insufficient to reproduce the X-ray spectrum of XTE J1118+480 and they had to reduce the mass accretion rate close to the black hole.

Specifically, they assumed that the mass accretion rate varies as a function of radius as $\dot{M}(r) \propto r^p$ and obtained adequate fits only for $p \geq 0.2$. The fate of the “missing mass” is not described in McClintock et al. (2003) but could possibly take the form of an outflow (e.g. Quataert & Narayan 1999), which is then like the ADIOS model (Blandford & Begelman 1999). This is also quite similar to Yuan et al. (2004), who added a jet contribution to the standard ADAF model in order to fit the spectral energy distribution of XTE J1118+480 in the hard state. Within this context, an X-ray power-law photon index of ~ 2 is predicted for BH in quiescence (Yuan & Cui 2005). However, at low luminosity the accretion flow is known to be convectively unstable (Igumenshchev & Abramowicz 1999; Quataert & Gruzinov 2000), and this convection-dominated accretion flow (CDAF) has a very different structure than the standard ADAF, as convection significantly reduces the mass accretion rate (equivalent to setting ADAF p parameter to 1 in eq. 1 of McClintock et al. 2003). In this CDAF framework, the X-ray spectra are expected to soften significantly at very low luminosity (Ball et al. 2001) as observed in our study. So, it is likely that ADAF models would be able to reproduce the soft and hard spectra described above, by tuning the amount of outflow or convection with the p parameter. To reproduce the harder spectra of longer orbital period systems, such as V404 Cyg, larger values of the p parameter, corresponding to stronger outflow or stronger convection, would be required.

Alternatively, in standard sphere+disk model, a softening of the X-ray spectra would also be expected due to a decrease of the coronal optical depth as the mass accretion rate decreases (see, for example, the discussion in Tomsick et al. 2004). In the magnetic corona model, active regions above the disk are responsible for producing the hard X-ray emission and constitute the base of the outflow (Merloni & Fabian 2002). In that model, the X-ray spectrum is expected to soften at lower accretion rate as the accretion power is carried away into the jets rather than being used to heat the electrons (Merloni & Fabian 2002). Such a model could easily explain the soft spectra of our sources in quiescence. However, in this model, the inner boundary of the accretion disk does not vary with mass accretion rate. The characteristic frequencies of QPOs and of broad-band timing noise are known to vary at state transitions and in the hard state (Tomsick et al. 2004; Kalemci et al. 2005), with lower frequencies generally occurring at lower luminosities. This is easy to understand in models where the inner disk radius increases at low mass accretion rates, but is difficult to explain in the models where the inner disk radius is constant.

Alternatively, a new possibility for the origin of X-ray emission has emerged in recent years. Indeed, a strong correlation is observed between the radio and X-ray emission of GX 339–4 and V404 Cyg in the hard state, and this correlation seems to extend down to the quiescent level for these two sources (Corbel et al. 2003; Gallo et al. 2003). The radio emission originates from a powerful self-absorbed compact jet (Corbel et al. 2000), and it

also seems possible that this jet may contribute to the high energy emission (Markoff et al. 2001, 2003) of BH in the standard hard state. Furthermore, radio observations show that the compact jet (at least for V404 Cyg) is maintained in quiescence (Gallo et al. 2004). Even if the debate is still open regarding the contribution of the compact jet (Markoff & Nowak 2004, Homan et al. 2005, Markoff et al. 2005) at high energy, we can check if the jet model could explain the softening of X-ray spectra for BH in quiescence. To explain the X-ray spectra in the hard state, the electron energy distribution should have an energy index of the order of 2.2–2.4 (Markoff et al. 2003). If the electrons that could be responsible for the X-ray emission of BH in quiescence are above the cooling break due to spectral ageing, then the energy index of the electron distribution (above the break) would be 3.2–3.4, therefore increasing (by 0.5) the photon index to $\Gamma \sim 2.1$ as observed in a large part of the sources from our sample. In this picture, the reason for the change would be that the particles are not sufficiently re-accelerated at low accretion rate, which is indeed quite reasonable. Alternatively, the compact jet contribution may vanish at low luminosity giving the possibility that thermal emission from the nozzle dominates the X-ray band and therefore gives a different spectral shape. The hard spectra ($\Gamma \sim 1.6$) would easily be explained if the compact jet properties are similar to the standard hard state. This is consistent with the fact that these kind of spectra are observed for the sources (V404 Cyg, GRO J1655–40 and V4641 Sgr) that have a large accretion disk, and which may be a necessary condition to sustain a powerful compact jet. Similarly, it is of some interest to note that acceleration processes are also believed to be inefficient in the jets of the low luminosity ($10^{-9} L_{\text{Edd}}$) supermassive black hole, Sgr A*, located in the center of our Galaxy (Melia & Falcke 2001).

5. Conclusions

We have observed and detected XTE J1550–564 and H 1743–322 during their quiescent states at their faintest level of X-ray emission with a 0.5–10 keV luminosity of 2×10^{32} $(d/5 \text{ kpc})^2 \text{ erg s}^{-1}$ for XTE J1550–564 and $9 \times 10^{31} (d/8 \text{ kpc})^2 \text{ erg s}^{-1}$ for H 1743–322. Such levels of X-ray emission are in the upper range compared with the levels observed in other black hole systems. The *Chandra* observations also provide the best constraint on the power-law index of XTE J1550–564 with an index of 2.25 ± 0.08 . We focused our analysis on the power-law model as this spectral shape is typically seen for black holes in quiescence and can represent an approximation for most theoretical emission mechanisms, but we emphasize that we can not statistically rule out other spectral shapes. All *Chandra* spectra of XTE J1550–564 are consistent with a soft power-law; therefore, indicating that the X-ray spectrum softens at lower luminosity. We bring to light that all systems with short orbital period ($\sim < 60$ hours) are consistent with a softening of their X-ray spectra in

quiescence. However, the long orbital period systems may be consistent with a hardening of their X-ray spectra, but confirmation of this trend is required. A possible and realistic test would be to obtain *XMM-Newton* or *Chandra* observations of long orbital period systems, like V4641 Sgr or GRO J1655–40 with a long exposure during quiescence. In addition, GRS 1915+105, with an orbital period of 833 hours, may be a very good target if it returns to quiescence. Simultaneously, further observations of short orbital period systems (like XTE J1650–500, or 4U 1543–47 at lower luminosity) should be performed in order to test the softening of their spectra. We found that various classes of models (ADAF corona + jet, CDAF, sphere+disk, magnetic corona or jet models) are able to reproduce the softening of the spectra in quiescence, but we note that most of them need the presence of powerful outflow or significant convection in order to reproduce these soft X-ray spectra. This may increase the likelihood that outflows are present in the most frequent phase (quiescence) of black hole binary’s activity and have significant influence on the physics of these systems and neighbouring environment (Fender et al. 2003, 2005).

S.C. would like to thank H. Falcke, R. Fender, A. King, E. Kording, and S. Markoff for discussions on various aspects of BH emission models. *RXTE*/ASM results are provided by *RXTE*/ASM team at MIT. We thank the anonymous referee for constructive comments. PK acknowledges partial support from NASA Chandra grants GO4-5038 and GO4-5039 and from a University of Iowa Faculty Scholar Award. JAT acknowledges partial support from NASA Chandra grant GO3-4041X.

REFERENCES

Ball, G. H., Narayan, R., & Quataert, E. 2001, ApJ, 552, 221
Bautz, M. W., Pivovaroff, M., Baganoff, F. et al. 1998, Proc. SPIE, 3444, 210
Blandford, R. D., & Begelman, M. C. 1999, MNRAS, 303, L1
Buxton, M. M., & Bailyn, C. D. 2004, ApJ, 615, 880
Campana, S., Parmar, A. N., & Stella, L. 2001, A&A, 372, 241
Cash, W. 1979, ApJ, 228, 939
Corbel, S., Fender, R. P., Tzioumis, A. K. et al. 2002, Science, 298, 196
Corbel, S., Nowak, M. A., Fender, R. P. et al. 2003, A&A, 400, 1007

Corbel, S., Fender, R. P., Tomsick, J. A. et al. 2004, *ApJ*, 617, 1272

Corbel, S., Kaaret, P. Fender, R. P. et al. 2005, *ApJ*, in press, astro-ph/0505526

Doxsey, R., Bradt, H., Fabbiano, G., et al. 1977, *IAU Circ.*, 3113

Ebisawa, K., Ogawa, M., Aoki, T. et al. 1994, *PASJ*, 46, 375

Fender, R. P., Maccarone, T. J., & van Kesteren, Z. 2005, *MNRAS*, 360, 1085

Fender, R. P., Gallo, E., & Jonker, P. G. 2003, *MNRAS*, 343, L99

Frank, J., King, A., & Raine, D. 1992, *Accretion Power in Astrophysics*, Cambridge University Press, 1992.

Frontera, F., Amati, L., Zdziarski, A. A. et al. 2003, *ApJ*, 592, 1110

Freeman, P. E., Kashyap, V., Rosner, R., & Lamb, D. Q. 2002, *ApJS*, 138, 185

Gallo, E., Fender, R. P., & Pooley, G. G. 2003, *MNRAS*, 344, 60

Gallo, E., Fender, R., & Corbel, S. 2003b, *The Astronomer's Telegram*, 196

Gallo, E., Fender, R. P., & Hynes, R. I. 2005, *MNRAS*, 356, 1017

Garcia, M. R., McClintock, J. E., Narayan, R. et al. 2001, *ApJ*, 553, L47

Gelino, D. M., Harrison, T. E., & Orosz, J. A. 2001, *AJ*, 122, 2668

Hameury, J.-M., Barret, D., Lasota, J.-P. et al. 2003, *A&A*, 399, 631

Hannikainen, D., Campbell-Wilson, D., Hunstead, R. et al., *Astrophysics and Space Science Supplement*, 276, 45

Hjellming, R. M., & Rupen, M. P. 1995, *Nature*, 375, 464

Homan, J., Buxton, M., Markoff, et al. 2005, *ApJ*, in press, astro-ph/0501349

Hynes, R. I., Steeghs, D., Casares, J. et al. 2004, *ApJ*, 609, 317

Hynes, R. I., Steeghs, D., Casares, J., Charles, P. A., & O'Brien, K. 2003, *ApJ*, 583, L95

Igumenshchev, I. V., & Abramowicz, M. A. 1999, *MNRAS*, 303, 309

Jain, R. K., Bailyn, C. D., Orosz et al. 1999, *ApJ*, 517, L131

Jain, R. K., Bailyn, C. D., Orosz et al. 2001, *ApJ*, 554, L181

Jonker, P.G., Gallo, E., Dhawan, et al. 2004, MNRAS, 351, 1359

Kaaret, P., Corbel, S., Tomsick, J. A. et al. 2003, ApJ, 582, 945

Kalemci, E., Tomsick, J. A., Buxton, M. M. et al. 2005, ApJ, 622, 508

Kaluzienski, L. J. & Holt, S. S. 1977, IAU Circ., 3099

Kong, A. K. H., Kuulkers, E., Charles, P. A., & Homer, L. 2000, MNRAS, 312, L49

Kong, A. K. H., McClintock, J. E., Garcia, M. R., Murray, S. S. & Barret, D. 2002, ApJ, 570, 277

Kotani, T., Kawai, N., Nagase, F. et al. 2000, ApJ, 543, L133

La Palombara, N., & Mereghetti, S. 2005, A&A, 430, L53

Markoff, S., Nowak, M., Corbel, S., Fender, R., & Falcke, H. 2003, A&A, 397, 645

Markoff, S., & Nowak, M. A. 2004, ApJ, 609, 972

Markoff, S., Nowak, M., Wilms, J. 2005, ApJ, in press

McClintock, J. E., & Remillard, R. A. 2004, in Compact Stellar X-ray sources, eds. W. H. G. Lewin & M. van der Klis, (Cambridge: Cambridge University Press), in press, astro-ph/0306213

McClintock, J. E., Narayan, R., Garcia, M. R. et al. 2003, ApJ, 593, 435

McClintock, J. E., Garcia, M. R., Caldwell, N., Falco, E. E., Garnavich, P. M., & Zhao, P. 2001, ApJ, 551, L147

Menou, K., Esin, A. A., Narayan, R. et al. 1999, ApJ, 520, 276

Melia, F., & Falcke, H. 2001, ARA&A, 39, 309

Merloni, A., & Fabian, A. C. 2002, MNRAS, 332, 165

Miller, J.M., Raymond, J., Homan, J. et al. 2005, ApJ, submitted, astro-ph/0406272

Nowak, M. A., Wilms, J., & Dove, J. B. 2002, MNRAS, 332, 856

Orosz, J. A. 2003, IAU Symposium, 212, 365

Orosz, J. A., Groot, P. J., van der Klis, M. et al. 2002, ApJ, 568, 845

Orosz, J. A., et al. 2001, *ApJ*, 555, 489

Quataert, E., & Gruzinov, A. 2000, *ApJ*, 539, 809

Quataert, E., & Narayan, R. 1999, *ApJ*, 520, 298

Revnivtsev, M., Chernyakova, M., Capitanio, F. et al. 2003, *The Astronomer's Telegram*, 132

Rupen, M. P., Mioduszewski, A. J., & Dhawan, V. 2003, *The Astronomer's Telegram*, 142

Sánchez-Fernández, C., Castro-Tirado, A.J., Duerbeck, H. W. et al. 1999, *A&A*, 348, L9

Shahbaz, T., Ringwald, F. A., Bunn, J. C., Naylor, T., Charles, P. A., & Casares, J. 1994, *MNRAS*, 271, L10

Smith, D. A. 1998, *IAU Circ.*, 7008

Swank, J. 2004, *The Astronomer's Telegram*, 301

Sutaria, F. K., Kolb, U., Charles, P. et al. 2002, *A&A*, 391, 993

Tomsick, J. A., Corbel, S., Kaaret, P. 2001, *ApJ*, 563, 229

Tomsick, J. A., Corbel, S., Fender, R.P. et al. 2003a, *ApJ*, 582, 933

Tomsick, J. A., Corbel, S., Fender, R.P. et al. 2003b, *ApJ*, 597, L133

Tomsick, J. A., Kalemci, E., & Kaaret, P. 2004, *ApJ*, 601, 439

Weisskopf, M. C., Brinkman, B., Canizares, C. et al. 2002, *PASP*, 114, 1

Wachter, K, Leach, R, & Kellogg E. 1979, *ApJ*, 230, 274

White, N. E., & Marshall, F. E. 1983, *IAU Circ.*, 3806

Yuan, F., Cui, W., & Narayan, R. 2005, *ApJ*, 620, 905

Yuan, F., & Cui, W. 2005, *ApJ*, in press, *astro-ph/0411770*

Table 1: *Chandra* observations of XTE J1550–564 and H 1743–322 : Best fitting spectral parameters for a power-law model. All quoted uncertainties are 90% confidence ($\Delta\chi^2 = 2.7$ for one parameter or $\Delta\chi^2 = 4.6$ for two parameters).

Source (Date)	Exposure (s)	Number ^a of counts	N_H (10^{22} cm $^{-2}$)	Photon index	χ^2_ν / dof	Cash ^b M.C. prob.	$F_{0.5-10 \text{ keV}}^c$ (10^{-14} ergs s $^{-1}$ cm $^{-2}$)
XTE J1550–564							
MJD 51777.4	4985	71	0.9 (fixed)	2.6 ± 0.4	–	0.57	26.6 ± 3.5
MJD 51798.3	4572	111	0.9 (fixed)	$2.3^{+0.5}_{-0.2}$	–	0.57	46.7 ± 4.7
MJD 52344.8	26118	1206	$0.86^{+0.19}_{-0.11}$	$2.20^{+0.25}_{-0.18}$	32.8/30	–	
			0.9 (fixed)	$2.25^{+0.10}_{-0.10}$	32.8/31	–	93.7 ± 2.8
MJD 52444.5	18025	58	0.9 (fixed)	$2.8^{+0.5}_{-0.9}$	–	0.55	6.8 ± 1.0
MJD 52542.0	24442	223	$0.90^{+0.53}_{-0.23}$	$2.2^{+0.7}_{-0.5}$	16.1/19	–	
			0.9 (fixed)	$2.23^{+0.25}_{-0.24}$	16.1/20	–	17.6 ± 1.2
MJD 52667.3	23683	254	$0.90^{+0.47}_{-0.22}$	$2.2^{+0.6}_{-0.4}$	13.9/19	–	
			0.9 (fixed)	$2.19^{+0.23}_{-0.21}$	13.9/20	–	21.3 ± 1.3
MJD 52935.6	47835	145	$0.69^{+0.47}_{-0.22}$	$2.2^{+0.7}_{-0.5}$	17.3/19	–	
			0.9 (fixed)	$2.5^{+0.4}_{-0.3}$	18.5/20	–	5.7 ± 0.5
Combined			$0.88^{+0.12}_{-0.09}$	$2.25^{+0.09}_{-0.13}$	137/167	–	
			0.9 (fixed)	2.25 ± 0.08	137/168	–	
H 1743–322							
			(10^{22} cm $^{-2}$)				(10^{-15} ergs s $^{-1}$ cm $^{-2}$)
MJD 53048.0	17796	6	2.3 (fixed)	$1.3^{+2.1}_{-1.7}$	–	0.33	
			2.3 (fixed)	2.0 (fixed)	–	0.48	12.2 ± 5.2
MJD 53088.9	28363	16	2.3 (fixed)	$1.6^{+1.0}_{-1.3}$	–	0.38	
			2.3 (fixed)	2.0 (fixed)	–	0.52	19.5 ± 5.3
MJD 53091.5	40037	52	2.3 (fixed)	2.2 ± 0.6	–	0.64	
			2.3 (fixed)	2.0 (fixed)	–	0.62	50.3 ± 7.3
Combined			2.3 (fixed)	1.96 ± 0.46	–	0.62	

^aNumber of total count within the source region in the 0.3–8 keV energy band

^bXSPEC Monte-Carlo simulations of 10,000 spectra based on the fitted model. We list the fraction of these simulated spectra that has a Cash statistic value less than the original data (for good fit, this number should be around 0.50).

^cUn-absorbed X-ray flux in the 0.5–10 keV energy band.

Table 2: Parameters of our sample of quiescent black holes: photon index and orbital parameters.

Source	Photon ^a Index (Γ)	Quiescent ^b		Orbital Period (hrs)	Distance ^c (kpc)	Primary ^d Mass (M_\odot)	Secondary ^c Mass (M_\odot)
		X-ray flux ($\text{erg s}^{-1} \text{ cm}^{-2}$)	Luminosity (L_{Edd})				
XTE J1118+480	2.02 ± 0.16	8.6×10^{-15} [1]	3.9×10^{-9}	4.08	1.8 ± 0.6 [1]	6.48–7.19	0.23–0.32
A 0620–00	2.26 ± 0.18	2.6×10^{-14} [1]	3.1×10^{-9}	7.75	1.16 ± 0.11 [2]	8.70–12.86	0.48–0.97
XTE J1550–564 ^e	2.25 ± 0.08	5.7×10^{-14} [2]	1.4×10^{-7}	37.03	5.3 ± 2.3 [3]	9.68–11.58	0.94–1.64
GX 339–4 ^f	1.99 ± 0.15	3.4×10^{-13} [3]	3.5×10^{-6}	42.00	> 6 [4]	5.8	0.52
GRO J1655–40	$1.30^{+0.34}_{-0.41}$	2.8×10^{-14} [4]	4.3×10^{-8}	62.92	3.2 ± 0.2 [5]	6.03–6.57	2.23–2.74
V4641 Sgr	0.2 ± 0.9	1.0×10^{-14} [5]	1.2×10^{-7}	67.61	9.6 ± 2.4 [6]	6.82–7.42	2.85–3.34
V404 Cyg	1.55 ± 0.05	8.9×10^{-13} [6]	6.5×10^{-7}	155.28	3.0 ± 0.8 [7]	10.06–13.38	0.53–0.83

^a90% confidence level. References in text. See also discussion on the influence of the hydrogen column density on the photon index.

^b0.5–10 keV unabsorbed X-ray flux. Adapted from quoted reference with PIMMS from Heasarc. 1: McClintock et al. 2003; 2: This work; 3: Gallo et al. 2003b; 4: Kong et al. 2002; 5: Tomsick et al. 2003; 6: Campana et al. 2001.

^c1: McClintock et al. 2001; 2: Gelino et al. 2001; 3: Orosz et al. 2002; 4: Hynes et al. 2004; 5: Hjellming & Rupen 1995; 6: Orosz et al. 2001; 7: Shahbaz et al. 1994.

^dEstimated 1 σ range from Orosz (2003) and references therein.

^eOrbital parameters from Orosz et al. (2002) taking into account the rotational velocity of the star.

^fOrbital parameters from Hynes et al. (2003)

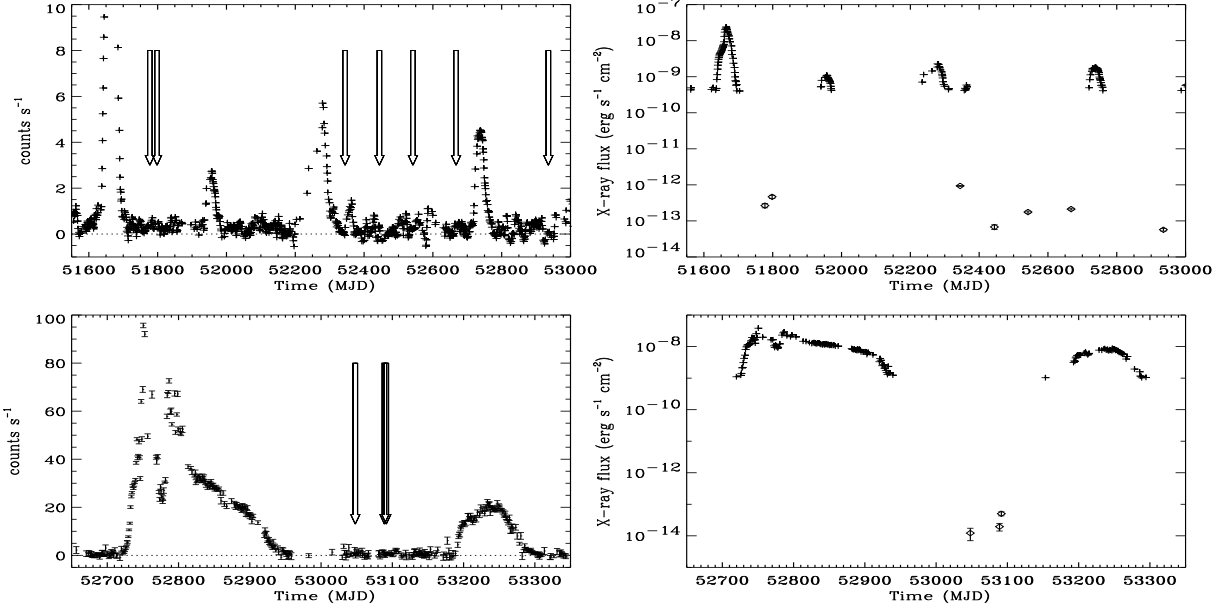


Fig. 1.— *RXTE*/ASM 1.5-12 keV light-curve of XTE J1550–564 (Left/top) and H 1743–322 (Left/bottom) covering the period of our *Chandra* observations. For the light-curve of XTE J1550–564, the points represent 5-day averages, highlighting the weaker outbursts observed in 2001, 2002 and 2003 (y-axis also truncated at 10 c/s for that purpose, the major outburst in 1998-99 is not shown also), whereas we plot daily averages for H 1743–322. The arrows mark the time of the *Chandra* observations which have all been conducted while the black holes were in (or close to) quiescence. In the panels on the right, the ASM 1.5-12 keV lightcurves are expressed directly ($75 \text{ ASM c.s}^{-1} = 1 \text{ Crab} = 3.0 \times 10^{-8} \text{ erg s}^{-1} \text{ cm}^{-2}$) in flux units in order to allow a direct comparison with the *Chandra* 0.5-10 keV un-absorbed flux measurements (diamond points). The apparent ASM detection of XTE J1550–564 around MJD 52360 is likely an artifact due to the location of the source close to the solar exclusion zone.

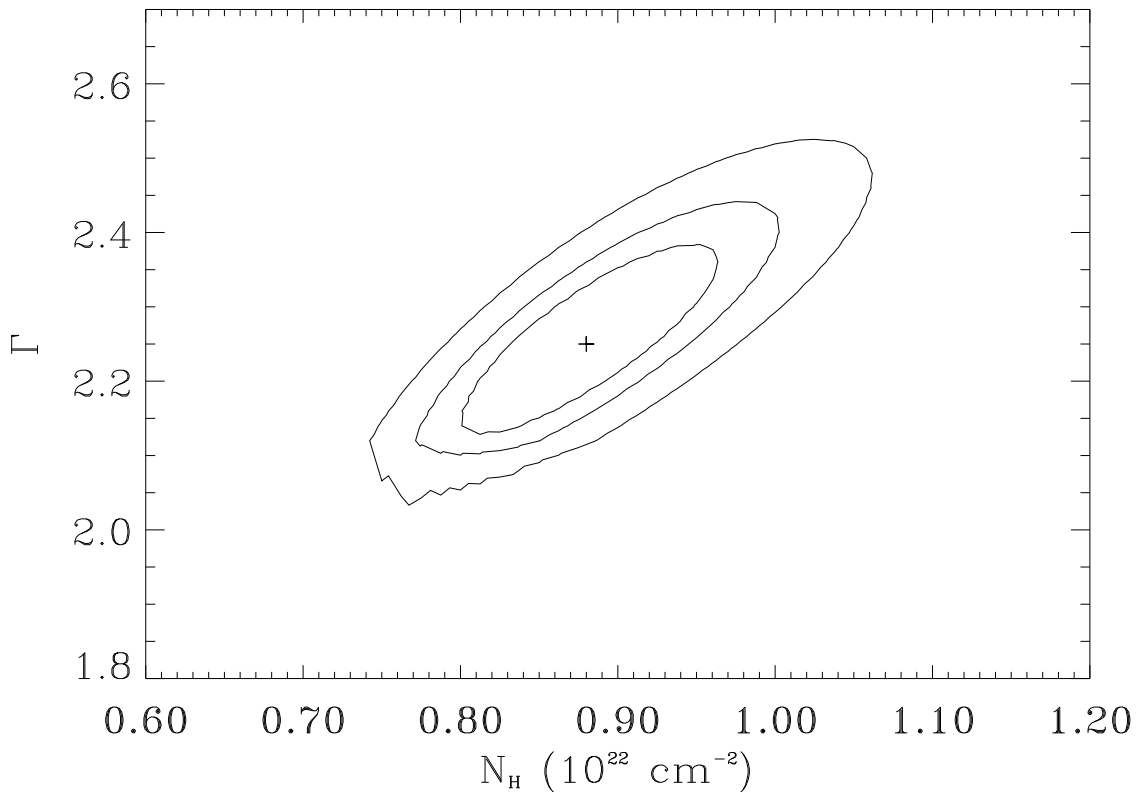


Fig. 2.— Error contours for the hydrogen column density (N_H) and the power-law index (Γ) derived from the combined *Chandra* spectrum of XTE J1550–564. The cross marks the location of the best-fit value, and 68% ($\Delta\chi^2 = 2.30$), 90% ($\Delta\chi^2 = 4.61$) and 99% ($\Delta\chi^2 = 9.21$) confidence contours are shown.

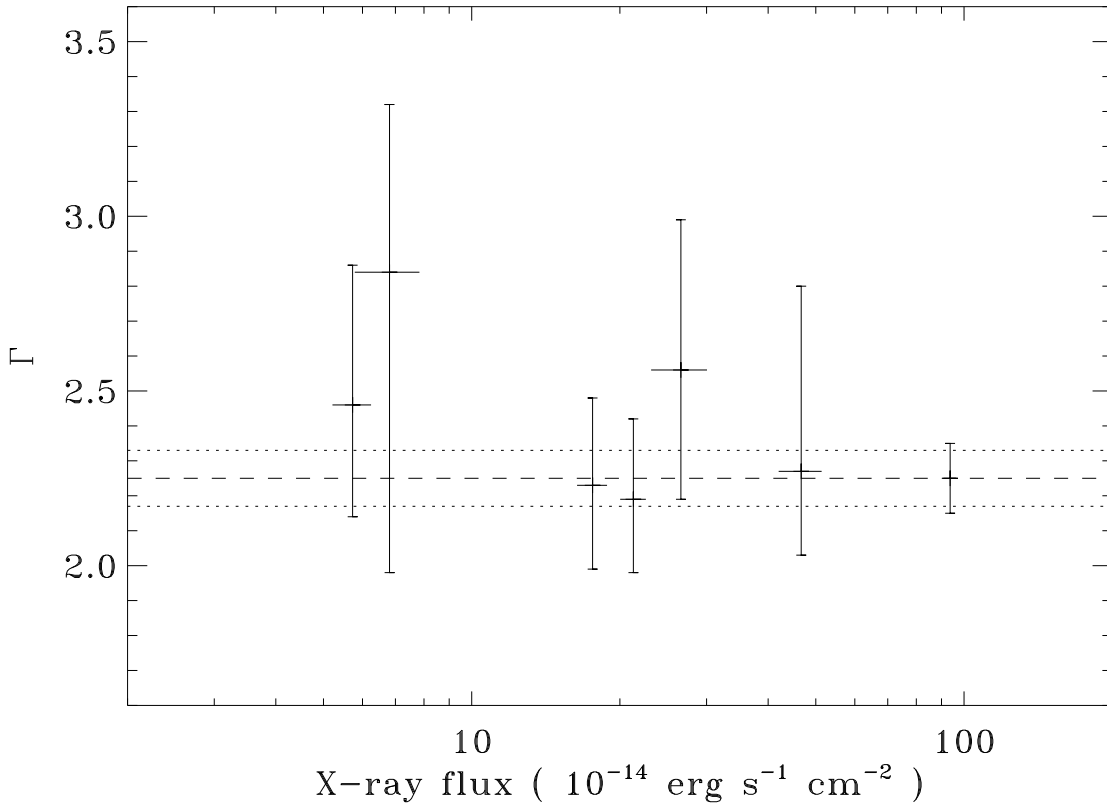


Fig. 3.— Evolution of the power-law photon index (Γ) versus the un-absorbed 0.5–10 keV flux for all *Chandra* observations of XTE J1550–564 in quiescence. The line indicates the best-fit value for Γ . All quoted errors are at the 90% confidence level.

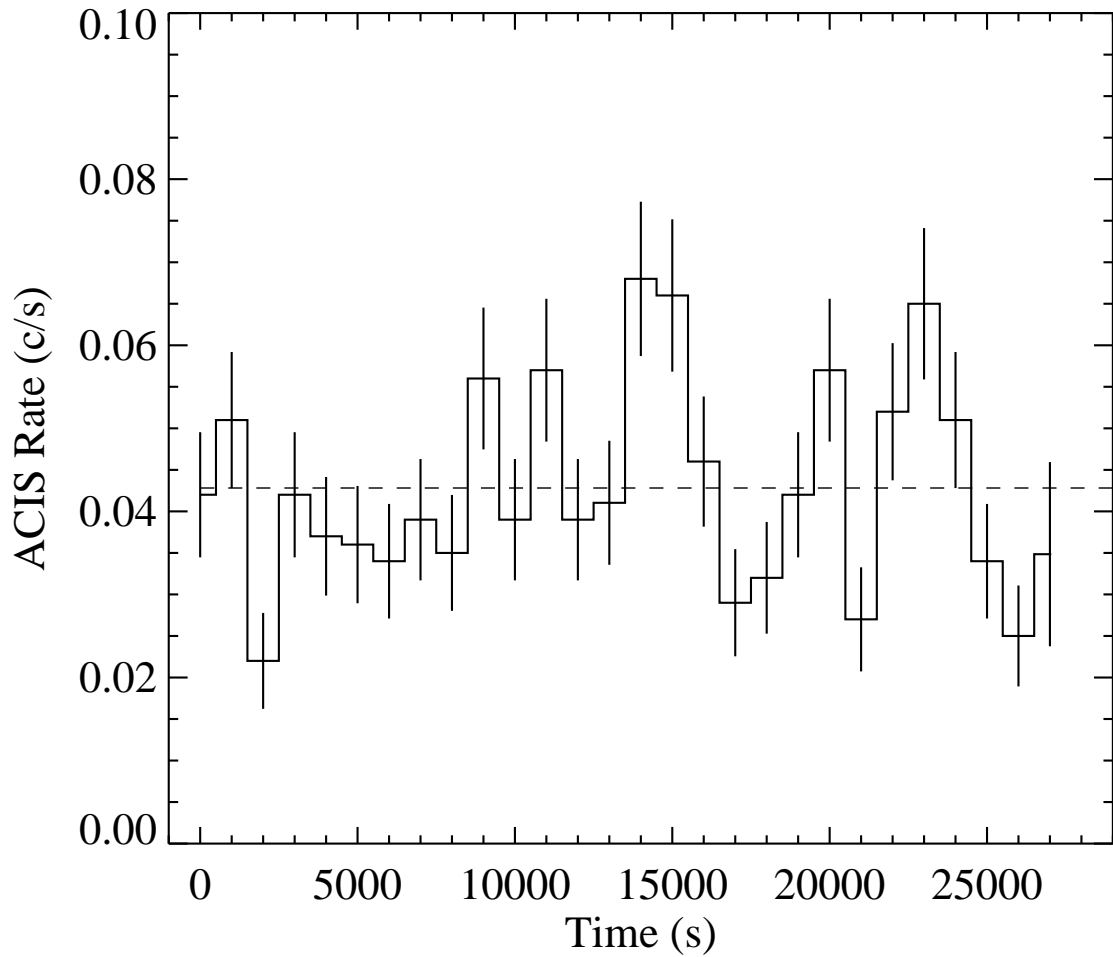


Fig. 4.— *Chandra* ACIS-S light-curve of XTE J1550–564 on MJD 52344 in the 0.3–8 keV band with a time resolution of 1 ks. The dashed line illustrates the fit with a constant level.

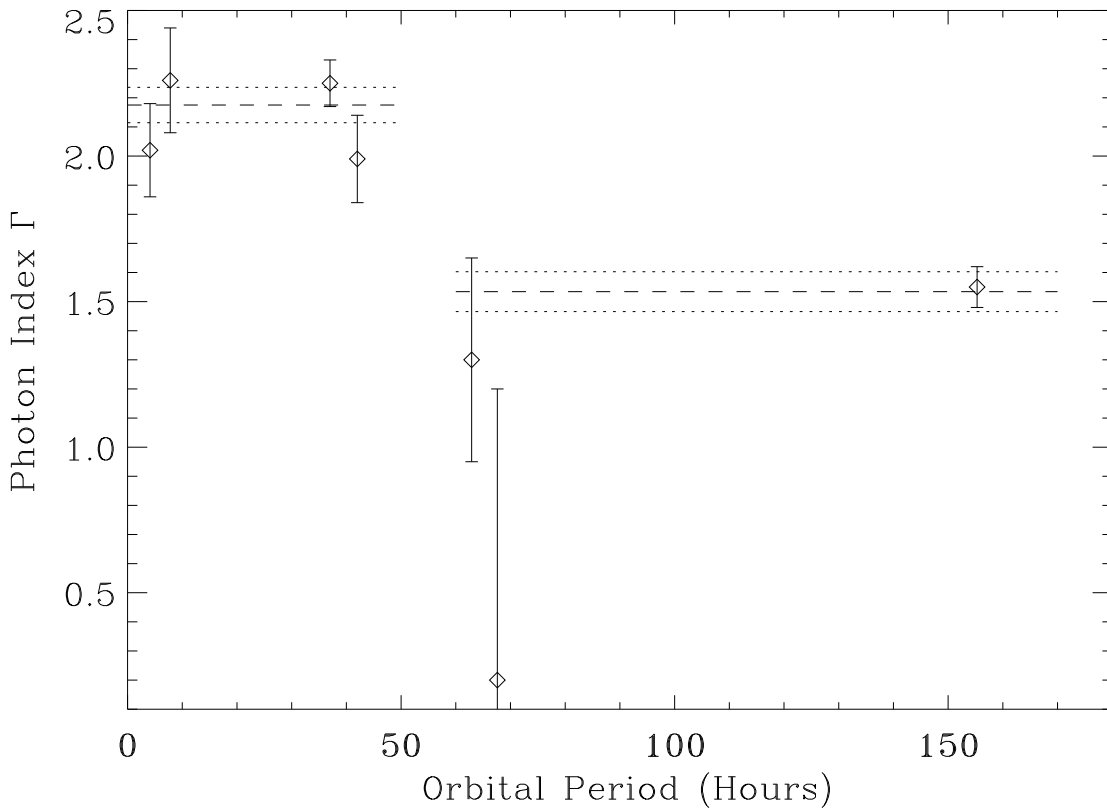


Fig. 5.— Evolution of the power-law photon index (Γ) versus orbital period for XTE J1118+480, A 0620–00, XTE J1550–564, GX 339–4, GRO J1655–40, V4641 Sgr, and V404 Cyg (in order of increasing orbital period) in their quiescent states. The lines (with associated 1σ error) indicate the average value of the photon index for the two groups (hard or soft – see text) of sources.

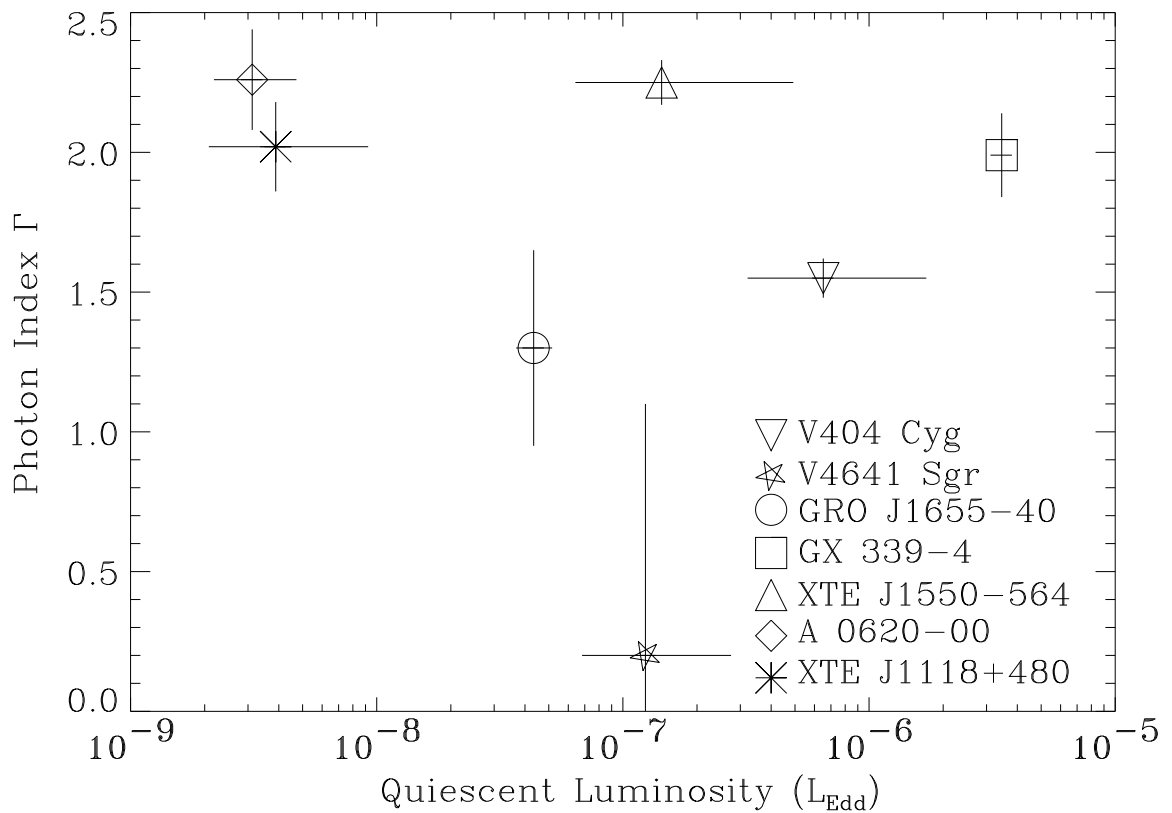


Fig. 6.— Evolution of the power-law photon index (Γ) versus the 0.5–10 keV quiescent luminosity (in Eddington units). The uncertainty in the luminosity is based on the uncertainty in the black hole mass and distance. A distance of 8 kpc associated with a mass of $6 M_{\odot}$ have been used for GX 339–4 (Hynes et al. 2003; 2004).